Site-Directed Mutagenesis, Kinetic, and Spectroscopic Studies of the P-Loop Residues in a Low Molecular Weight Protein Tyrosine Phosphatase[†]

Bornadata Evans, Patrick A. Tishmack, Christine Pokalsky, Marie Zhang, and Robert L. Van Etten*

Department of Chemistry, Purdue University, West Lafayette, Indiana 47907-1393

Received March 7, 1996; Revised Manuscript Received July 3, 1996[⊗]

ABSTRACT: The structure of the specific phosphate binding loop (P-loop) of bovine protein tyrosine phosphatase (BPTP) is very similar to that present in high M_r PTPases. Site-directed mutagenesis was used to explore the role of several conserved residues involved in forming the P-loop of BPTP. Thus, Ser-19 and Ser-43 were individually mutated to alanines, and Asn-15 was mutated to alanine and glutamine. The ^{1}H NMR spectra of the mutants showed good conservation of global secondary structure when compared to wild-type enzyme. Kinetic measurements revealed that only S19A and N15A had substantially altered catalytic activities toward *p*-nitrophenyl phosphate at pH 5.0, with both mutants exhibiting V_{max} values that were 0.25−0.33% of wild-type enzyme. Further kinetic analyses of the N15A and S19A mutants were performed using phosphomonoester substrates with varied phenolic leaving groups. For S19A, the slope of the correlation between V_{max} and the substrate leaving group pK_a was significantly altered, consistent with a change of the rate-determining step from dephosphorylation to phosphorylation. This was confirmed by partitioning experiments employing methanol as an alternative nucleophile in the dephosphorylation step. Thus, mutating Ser-19 to alanine reduced the efficiency of nucleophilic attack by Cys-12. It is concluded that Ser-19 acts to facilitate the ionization and orientation of Cys-12 for optimal reaction as a nucleophile and as a leaving group. It also appears that Asn-15, Ser-19, His-72, and to a lesser extent Ser-43 serve structural functions that allow the active site to adopt an optimal geometry for phosphate binding. The Asn-15 to Ala mutation appears to disrupt the hydrogen-bonding network, with an accompanying alteration of the geometry of the P-loop. These conclusions are also consistent with changes in the stability of the respective proteins, as measured by urea denaturation.

Many cellular processes are regulated through the reversible phosphorylation of proteins. This reversible phosphorylation is catalyzed by groups of proteins known as kinases and phosphatases (Fischer *et al.*, 1991; Cohen, 1992). Phosphorylation of tyrosines is involved in many of these regulatory mechanisms (Edelman *et al*., 1987; Cohen, 1989; Fischer *et al.*, 1991). There are several families of phosphotyrosyl phosphatases (PTPases)[1] including receptor-like and cytoplasmic high molecular weight phosphatases (Charbonneau & Tonks, 1992; Zhang & Dixon, 1994). Although very diverse in size and structural organization, the members of this gene family generally possess a conserved 240-residue segment that has been suggested to comprise an independently folding catalytic domain (Charbonneau & Tonks, 1992). A distinct class of soluble, cytoplasmic low molecular weight PTPases (M_r ≈18 000) is found in mammals, yeast, and bacteria (Heinrikson, 1969; Rehkop & Van Etten, 1975; Chernoff & Li, 1985; Okada *et al*., 1986; Waheed *et al*., 1988; Zhang & Van Etten, 1990; Ostanin *et al*., 1995). Bovine PTPase (BPTP), recently cloned and expressed in this laboratory, is a prototypical example of a low molecular weight PTPase (Wo *et al.*, 1992a). The mammalian enzymes are highly similar in sequence and exhibit 85−95% sequence identity, even though many of the vertebrate low molecular weight PTPases, including the human (Wo et al., 1992b) and rat liver enzymes, exist as isoenzymes. The extent of similarity between the mammalian and yeast forms of these enzymes is also relatively high, approximately 40% (Figure 1). Except for a CXXXXXR motif at the catalytic site (*vide infra*), the low molecular weight phosphotyrosyl phosphatases show no apparent sequence homology to the high molecular weight PTPases.

Analysis of the primary structure of the low molecular weight PTPases identified a motif that is similar to, but distinct from, the one known for the high molecular weight enzymes. In the high molecular weight PTPases, a conserved signature sequence, HCXAGXGR(S/T), is usually found in the C-terminal third of the protein (Zhang & Dixon, 1994). A related invariant motif, XCXXXXCRS, is found in the low molecular weight PTPases, where it is located close to the N-terminus. The histidine residue and glycine-rich nature of the phosphate binding loops that are found in the high molecular weight enzymes are not present in the small enzymes, but the placement of the serine and the catalytically critical cysteine and arginine residues is identical in both

[†] This work was supported by U.S. Department of Health and Human Services Research Grant GM-27003.

* To whom correspondence should be addressed. FAX: (317) 494-0239.

[⊗] Abstract published in *Advance ACS Abstracts,* October 1, 1996.

[1] Abbreviations: BPTP, bovine protein tyrosine phosphatase; CD, circular dichroism; D_2O, deuterium oxide; DSS, 2,2-dimethyl-2-silapentane-5-sulfonate; ΔG_{H_2O}, free energy change for unfolding in water without denaturant; $\Delta(\Delta G)$, difference in free energy change; IPTG, isopropyl β-D-thiogalactopyranoside; k_{cat}, catalytic rate constant or turnover number; K_i, inhibition constant; K_m, Michaelis constant or substrate concentration at half V_{max}; K_s, equilibrium binding constant; P-loop, the phosphate binding loop of BPTP, consisting of the sequence CLGNICRS; *p*NPP, *p*-nitrophenyl phosphate; PTPase, protein tyrosine phosphatase; SDS−PAGE, sodium dodecyl sulfate−polyacrylamide gel electrophoresis; SP-Sephadex, sulfopropyl-Sephadex; TFA, trifluoroacetic acid; V_{max}, enzyme velocity at saturating concentrations of substrate; WT, wild-type BPTP.

S0006-2960(96)00565-X CCC: $12.00 © 1996 American Chemical Society

```
BHPTP      AEQVTKSV--LFVCLGNICRSPIAEAVFRKLVTDQNISDNW-VIDSGAVS   47
HCPTPA     AEQATKSV--LFVCLGNICRSPIAEAVFRKLVTDQNISENW-RVDSAATS   47
HCPTPB     AEQATKSV--LFVCLGNICRSPIAEAVFRKLVTDQNISENW-VIDSGAVS   47
RATACP1    AEVGSKSV--LFVCLGNICRSPIAEAVFRKLVTDENVSDNW-RIDSAATS   47
RATACP2    AEVGSKSV--LFVCLGNICRSPIAEAVFRKLVTDENVSDNW-AIDSSAVS   47
Ltp1       MTIEKPKISVAFICLGNFCRSPMAEAIFKHEVEKANLENRFNKIDSFGTS   50
Stp1       MT---KNIQVLFVCLGNICRSPMAEAVFRNEVEKAGLEARFDTIDSCGTG   47
ERWINIA    MINS-----ILVVCIGNICRSPTGERLLKAALP----ERK---IASAGLK   38
                       *  *  **

BHPTP      DWNVGRSPDPRAVSCLRNHGINTA-HKARQVTKEDFVTFDYILCMDESNL   96
HCPTPA     GYEIGNPPDYRGQSCMKRHGIPMS-HVARQITKEDFATFDYILCMDESNL   96
HCPTPB     DWNVGRSPDPRAVSCLRNHGIHTA-HKARQITKEDFATFDYILCMDESNL   96
RATACP1    TYEVGNPPDYRGQNCMKKHGIHMQ-HIARQITREDFATFDYILCMDESNL   96
RATACP2    DWNVGRPPDPRAVNCLRNHGISTA-HKARQITREDFATFDYILCMDESNL   96
Ltp1       NYHVGESPDHRTVSICKQHGVKIN-HKGKQIKTKHFDEYDYIIGMDESNI   99
Stp1       AWHVGNRPDPRTLEVLKKNGIHTK-HLARKLSTSDFKNFDYIFAMDSSNL   96
ERWINIA    AM-VGGSADETASIVANEHGVSLQDHVAQQLTADMCRDSDLILVMEKKHI   87
                                   *

BHPTP      RDLNRKSNQVKNCRAKIELLGSYDPQK---QLIIEDPYYGNDADFETVYQ  143
HCPTPA     RDLNRKSNQVKTCKAKIELLGSYDPQK---QLIIEDPYYGNDSDFETVYQ  143
HCPTPB     RDLNRKSNQVKTCKAKIELLGSYDPQK---QLIIEDPYYGNDSDFETVYQ  143
RATACP1    RDLNRKSNQVKNCKAKIELLGSYDPQK---QLIIEDPYYGNDSDFEVVYQ  143
RATACP2    RDLNRKSNQVKNCKAKIELLGSYDPQK---QLIIEDPYYGNDSDFEVVYQ  143
Ltp1       NNLKKI--QPEGSKAKVCLFGDWNTNDGTVQTIIEDPWYGDIQDFEYNFK  147
Stp1       RNINRV--KPQGSRAKVMLFGEYASPG--VSKIVDDPYYGGSDGFGDCYI  142
ERWINIA    DLVCRINPSVRG---KTMLFGHWI-----NQQEIADPYKKSRDAFEAVYG  129
                                        *

BHPTP      QCVRCCRAFLEK-----VR                                  157
HCPTPA     QCVRCCRAFLEK-----AH                                  157
HCPTPB     QCVRCCRAFLEK-----AH                                  157
RATACP1    QCLRCCKAFLEK-----TH                                  157
RATACP2    QCLRCCKAFLEK-----TH                                  157
Ltp1       QITYFSKQFLKK-----EL                                  161
Stp1       QLVDFSQNFLKS-----IA                                  156
ERWINIA    VLENAAQKWVNALSR----                                  144
```

FIGURE 1: Sequence alignment of low molecular weight tyrosine phosphatases from bovine (BPTP), human (HCPTP A and B isoenzymes), rat (ACP 1 and 2 isoenzymes), *Saccharomyces cerevisiae* (Ltp1), and *Schizosaccharomyces pombe* (Stp1). Important catalytic and structural residues are marked with an asterisk (*), and conserved residues are shown in bold type.

Bovine Low M$_r$ PTPase	V	L	F	V	**C**	L	G	N	I	C	**R**	**S**	P
Human cdc 25	I	V	F	H	**C**	E	F	S	S	E	**R**	**G**	P
Human LAR PTPase	M	V	V	H	**C**	S	A	G	V	G	**R**	**T**	G
Human PTPase 1B	V	V	V	H	**C**	S	A	G	I	G	**R**	**S**	G
Human T-cell PTPase	A	V	I	H	**C**	S	A	G	I	G	**R**	**S**	G
Yersinia PTPase	P	V	I	H	**C**	R	A	G	V	G	**R**	**T**	A

FIGURE 2: Sequence alignment of the active site phosphate binding loop region of the bovine low molecular weight PTPase with other types of PTPases.

motifs, consistent with a common catalytic mechanism between the high and low molecular weight enzymes (Figure 2). Although the low molecular weight PTPases do not contain the glycine-rich GXGXXG phosphate binding motif that is present in many proteins including kinases, dehydrogenases, and many high molecular weight PTPases (Schultz, 1992), it is clear that the phosphate binding loop in BPTP provides equivalent phosphate binding ability.

The crystal and solution structures of BPTP have been determined (Zhang, M., *et al*., 1994; Logan *et al.*, 1994; Su *et al.*, 1994), and the X-ray crystallographic structure has recently been extended to 1.8 Å (Zhang *et al*., 1995). This high-resolution structure allows us to examine the relationship between the conserved sequence residues in the structure and the activity of the enzyme. Aided by the presence of the phosphate ion at the active site in the crystal structure, we can now define the residues that are important for the substrate binding and formation of the active site. Importantly, the backbone arrangement of the P-loop in BPTP is effectively identical to that found in the structure of a representative high M_r PTPase from *Yersinia*, with Cα positions exhibiting only 0.37 Å root mean square deviation (Stuckey *et al*., 1994; Zhang *et al*., 1995). Thus, despite apparent differences in the consensus sequences, the phosphate binding regions of these proteins are surprisingly similar.

The high-resolution structure of BPTP shows that several of the completely conserved residues are involved in the formation of the active site. The conserved asparagine (Asn-15), histidine (His-72), and two serines (Ser-19 and -43) are at or near the active site. His-72, Ser-19, and Ser-43 interact with the Asn-15 residue of the active site loop. The interaction of these three residues with Asn-15 evidently stabilizes the conformationally strained orientation (left-handed α-helical conformation) of the latter residue and modifies the structural orientation of the backbone so that all the NH groups in the active site loop are oriented toward the phosphate ion. The hydrogen bonds between His-72, Ser-19, Ser-43, and Asn-15 appeared to serve a structural function such that the active site loop could adopt the most favorable geometry for phosphate binding (Figure 3). Such positioning would not only explain earlier results from mutagenesis and spectroscopic studies of histidine mutants (Davis *et al.*, 1994a) but would also identify a role for the conserved serine and asparagine residues in the low molecular weight enzyme. The Ser-19 residue also forms a hydrogen bond with the nucleophilic cysteine, Cys-12 (Zhang *et al*., 1995). Consequently, Ser-19 may serve an additional role in the stabilization and orientation of this catalytically critical residue (Davis *et al.*, 1994b). The present study examines these possibilities.

EXPERIMENTAL PROCEDURES

Materials. Oligonucleotides were purchased from Integrated DNA Technologies. The M13 mutagenesis kit was purchased from U.S. Biochemical Co. The pET expression vector and *Escherichia coli* strains were from Novagen. Restriction enzymes were from New England Biolabs. *p*-Nitrophenyl phosphate, *β*-naphthyl phosphate, and phenyl phosphate were from Sigma. The remaining substrates were synthesized as previously described (Zhang *et al.*, 1991). Deuterium oxide (99.8%) and 2,2-dimethyl-2-silapentane-5-sulfonate (DSS) were obtained from Cambridge Isotope Laboratories. Ultrapure urea was obtained from U.S. Biochemical Co. Molecular modeling studies were done using the high-resolution crystal structure PDB file 1PNT from the Brookhaven Protein Database (Zhang, M., *et al*., 1994).

BPTP Mutagenesis and DNA Sequencing. Mutant proteins were obtained by site-directed mutagenesis (Vandeyar *et al.*, 1988) of the wild-type BPTP coding sequence (Wo *et al.*, 1992). A 765 bp *Xba*I−*Bam*HI fragment containing the BPTP gene (Wo *et al.*, 1992) was digested from the PVEBH4 vector and subcloned into the corresponding sites of the bacteriophage M13mp18. Mutagenesis was performed using the T7-Gen *in vitro* mutagenesis kit from U.S. Biochemical Co. The mutant gene was digested using *Xba*I−*Bam*HI restriction enzymes and subcloned into the pET11d expression vector. The ligation mixture was transformed into the *E. coli* strain DH5α. Individual colonies were selected for sequencing analysis to confirm the presence of the desired mutation. Single-stranded and double-stranded sequencing were performed using the Sanger dideoxy chain termination method (Sanger *et al.*, 1977) according to the manufacturer's protocol for Sequenase Version 2.0. Single base pair sequencing in M13mp18 (nucleotide tracking) was performed for initial confirmation of the desired mutation. The complete nucleotide sequence of the BPTP mutant was subsequently determined in the final construct to verify the

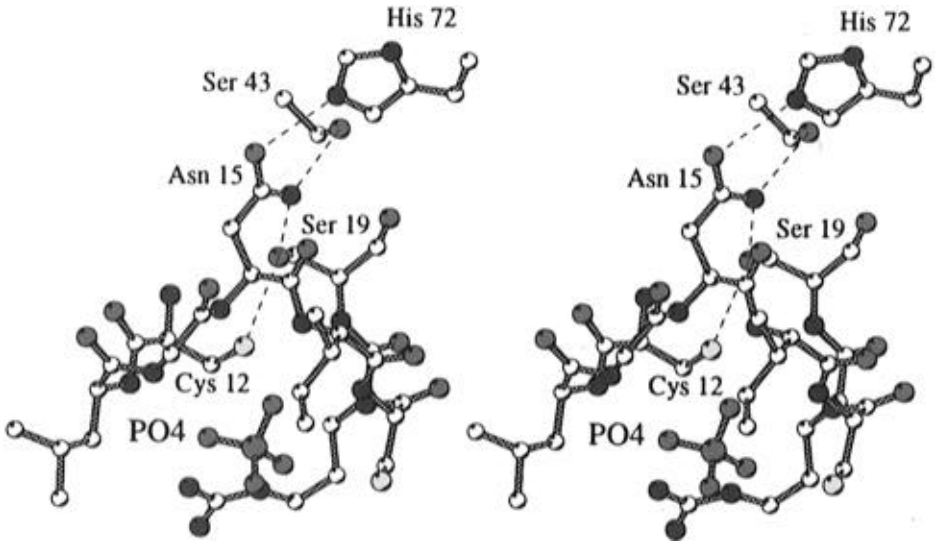

FIGURE 3: Stereoview of the active site of BPTP showing residues Ser-19, Ser-43, and His-72 that interact with Asn-15 to stabilize the conformation of the active site loop.

integrity of the full sequence. The *E. coli* BL21(DE3) strain was used for protein expression.

Expression and Purification of BPTP Mutants. Prior to large-scale purification of the mutants, small-scale experiments were performed to confirm expression of the correct size proteins. An overnight culture of BL21(DE3) carrying the mutant plasmid was diluted 1:10 in LB medium containing 50 μg/mL ampicillin. The cells were grown at 37 °C until the $OD_{600} = 0.8-1.0$. BPTP expression was induced by addition of 0.4 mM IPTG. After 3 h, the cells were harvested from 1.5 mL of culture by centrifugation for 5 min in a microcentrifuge. The cells were lysed by a lysozyme freeze/thaw procedure (Wo *et al.*, 1992). Crude extracts were then subjected to SDS−PAGE analysis (Laemmli, 1970) using a 12% gel with Coomassie Brilliant Blue R-250 staining. Large-scale expression of wild-type and mutant forms of BPTP was followed by a two-step purification scheme involving ion-exchange and gel permeation chromatography (Davis *et al.*, 1994b).

Reverse-Phase High-Pressure Liquid Chromatography. The purity of the resulting proteins was assessed by HPLC using an IBM LC/9533 ternary gradient liquid chromatograph equipped with an IBM LC/9523 variable-wavelength detector. Enzyme (10−20 μg) was loaded on a Synchropak RP-P C18 column and eluted with a linear gradient of 2−62% acetonitrile (containing 0.1% trifluoroacetic acid) for 60 min.

Circular Dichroism and ^{1}H NMR Spectroscopy. The CD spectra of wild-type and mutant proteins were measured on a JASCO Model J600 spectropolarimeter over the range 190−240 nm using a 2 mm cell. Proteins were prepared as 7 μM solutions in 10 mM sodium phosphate buffer at pH 5.0. One-dimensional ^{1}H NMR spectra were obtained with a Varian Unity Plus spectrometer operating at 14 T (600 MHz for ^{1}H). Protein samples (10−15 mg) were purified by the two-step procedure stated above and concentrated to <1 mL in a 10 mL Amicon stirred cell ultrafiltration device at 4 °C using a 25 mm YM3 membrane filter. The buffer was exchanged by ultrafiltration three times with a solution of 90% H_2O, 10% D_2O, and 150 mM NaCl. After the buffer was exchanged, the pH was between 5.2 and 5.8, and it was not adjusted further to avoid loss of protein due to precipitation. The final protein concentration was approximately 1.5 mM except for S43A, which was only 0.25−0.5 mM as a result of precipitation during buffer exchange. All spectra were obtained using Wilmad 528-PP 5 mm NMR tubes. The temperature was controlled at the probe to be 25 ± 1 °C. All spectra were obtained with 2 s acquisition time, 2 s relaxation delay, 64 acquisitions (256 for S43A), and 7200 Hz spectral width and processed with 64K points and 0.1 s Gaussian apodization function. The intense H_2O signal was suppressed by applying an 80−90 Hz radio-frequency field during the relaxation delay. Further suppression was done with the Varian solvent suppression algorithm to remove low-frequency signals. The H_2O resonance was set to 4.77 ppm versus DSS at 25 °C as an external reference standard.

Urea Denaturation Studies. Defined volumes of concentrated urea and enzyme stock solutions were diluted using 100 mM sodium acetate buffer, pH 5.0, and 80 mM NaCl to obtain final urea concentrations of 0−8 M. The wild-type enzyme concentration was 0.12 mg/mL, and similar protein concentrations were used for each of the mutant studies. Solutions were equilibrated for 2 h and maintained at 25 °C for the duration of the study. Intrinsic fluorescence intensities of enzyme samples in a 1 cm quartz cuvette were monitored using a Hitachi F2000 spectrofluorometer with an excitation wavelength of 295 nm, an emission wavelength of 320 nm, and slit widths of 5 nm (Pokalsky *et al.*, 1995).

Enzymatic Activity Assay. Phosphatase activity was measured at 37 °C with 10 mM *p*-nitrophenyl phosphate (*p*NPP) as a substrate in 100 mM sodium acetate buffer, pH 5.0, and an ionic strength adjusted to 150 mM by addition of sodium chloride (Zhang & Van Etten, 1990). Protein concentrations were determined by UV absorbance measurement at 280 nm using extinction coefficients previously measured at this wavelength (Davis *et al.*, 1994b).

Steady-State Kinetics. Michaelis−Menten parameters for wild-type BPTP and mutant proteins were determined using *p*NPP and phenyl phosphate in 100 mM sodium acetate buffer at pH 5.0. For V_{max} and K_m measurements, eight different substrate concentrations were used, ranging from 0.1 to 10 K_m, and triplicate measurements were made. The values were fitted to the Michaelis−Menten equation using the computer program Scientist (MicroMath, Inc.). Inhibition constants for inorganic phosphate were determined at pH

5.0 and 37 °C using eight different *p*NPP concentrations (0.1−10 K_m). The kinetic data were obtained without inhibitor and at four different inhibitor concentrations.

Hydrolysis of Aryl Phosphomonoesters. The k_{cat} and K_m values were determined for the N15A, N15Q, S19A, S43A, H72A, and R58A mutants with the following five aryl phosphomonoester substrates: 4-nitrophenyl, 4-(trifluoromethyl)phenyl, 4-ethylphenyl, β-naphthyl, and phenyl phosphate. The assays were carried out in pH 5.0 assay buffer at 37 °C. Duplicate or triplicate aliquots were taken at intervals over a 6 min period, and the initial velocities of the hydrolysis reaction were measured by determining the inorganic phosphate produced during the reaction (Black & Jones, 1983).

Partitioning Experiments. These experiments were carried out at 37 °C in 100 mM assay buffer in the presence of 0−2 M methanol, using *p*NPP as a substrate. The reaction was initiated by adding a catalytic amount of enzyme, and 4 min assays were performed. Duplicate or triplicate measurements were made. The initial velocities were measured by the amount of *p*-nitrophenolate and inorganic phosphate produced.

pH-Rate Profiles. Assay buffers used in the pH dependence studies were 100 mM formate (pH 3.0−3.9), 100 mM sodium acetate (pH 4.0−5.5), 100 mM citrate (pH 5.6−7.0), 50 mM diethyl malonate (pH 6.8−7.8), and 100 mM glycinamide (pH 7.9−8.9). All buffers contained 1 mM EDTA and were adjusted to an ionic strength of 150 mM using sodium chloride. At least ten different substrate (*p*NPP) concentrations ranging from 0.1 to 10 K_m were prepared for each pH, and the initial velocities of the enzyme-catalyzed hydrolysis reactions were measured at 37 °C. The kinetic parameters k_{cat} and K_m were determined from a nonlinear least squares analysis of the Michaelis−Menten equation using Scientist (MicroMath, Inc.). The pH data were fit to eq 1 or 2 depending upon the shape of the profile (Denu & Dixon, 1995). For eq 1 and 2, v_c is the pH-independent value of k_{cat}/K_m, H is the proton concentration, and K_{a1}, K_{a2}, and K_{a3} are the equilibrium constants for ionization of groups affecting k_{cat}/K_m. Fitting of the pH-dependent data to eq 1 or 2 was accomplished with nonlinear least squares analysis using Scientist (MicroMath, Inc.).

$$v = v_c/[(1 + H/K_{a1})(1 + K_{a2}/H)\,(1 + H/K_{a3})] \quad (1)$$

$$v = v_c/[(1 + H/K_{a1})(1 + K_{a2}/H)] \quad (2)$$

RESULTS

Overexpression and Purification of Enzymes. Large-scale expression of the N15Q, S43A, and R58A mutants produced 25−50 mg of enzyme/2 L of culture using the same purification procedure as that employed for the wild-type protein. However, the N15A and S19A mutants were more difficult to purify because the mutant proteins did not bind adequately to the SP-Sephadex C-50 cation-exchange column under similar conditions. These proteins were eventually purified using a lower ionic strength buffer consisting of 10 mM sodium acetate, 10 mM sodium phosphate, and 1 mM EDTA, pH 4.8. After this chromatographic step, the main impurity was a 29 kDa protein, β-lactamase. This was removed by passing the protein through a Sephadex G-50 size exclusion column. In each case, the protein was estimated to be >90% pure by reverse-phase high-pressure liquid chromatography or SDS−PAGE.

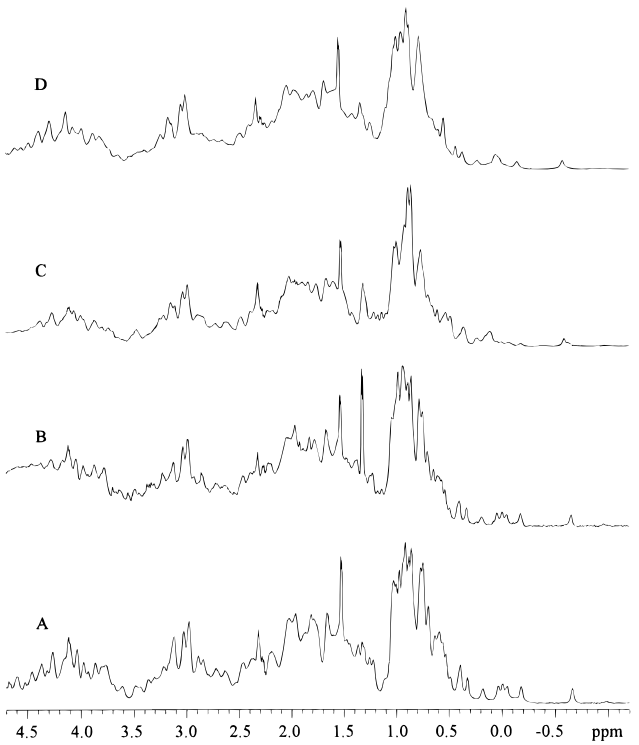

FIGURE 4: Comparison of 600 MHz ^{1}H NMR spectra for (A) WT, (B) S43A, (C) N15A, and (D) S19A BPTP in 90% H_2O, 10% D_2O, and 150 mM NaCl, pH 5.2−5.8, at 25 °C.

Circular Dichroism and NMR Analysis. In order to confirm the structural integrity of the mutants, CD and ^{1}H NMR spectra were obtained for several of the mutants that possessed reduced activity compared to wild-type protein. The CD spectra of the mutant proteins, measured over a range of 190−240 nm, showed no significant differences from that of the wild-type protein (data not shown). Previous NMR work had established the backbone ^{1}H, ^{13}C, and ^{15}N assignments (Zhou *et al*., 1994) and the complete solution structure (Logan *et al*., 1994) for wild-type enzyme. In the present study, one-dimensional ^{1}H NMR spectra were obtained to assess whether the protein secondary and tertiary structures were significantly altered by the various mutations. Figure 4 shows a series of ^{1}H NMR spectra comparing the wild-type enzyme with three of the mutants (N15A, S19A, and S43A) that were examined in this study. A qualitative inspection of peak position and line shape of the resonances in wild-type and mutant BPTPs showed good conservation of global secondary structure for the mutants (Wishart *et al*., 1991a,b; Wishart & Sykes, 1994). The chemical shift dispersion in native state proteins is larger (i.e., resonances are observed ≤0.5 and ≥9 ppm) than for completely or partially denatured proteins. The spectra of N15A and S19A revealed only minor changes in the region of −0.7 to 0.5 ppm, which are indicative of small structural changes in these mutants. The S43A spectrum was nearly identical to that of wild-type BPTP in this region. Previous studies of wild-type enzyme showed that these low-frequency peaks were due to several hydrophobic amino acid side chain residues near the active site of BPTP. These residues are Val-8, Leu-9, and Val-11, which precede the Cys-12 nucleophile in the first β-strand in BPTP, and Ile-88 and Leu-89, which are part of a β-strand running parallel to the first β-strand (Zhang,

Table 1: Kinetic Parameters of WT and Mutant BPTP Using *p*NPP and Phenyl Phosphate as Substrates[a]

	*p*NPP		phenyl phosphate	
enzyme	K_m (mM)	V_{max} (units/mg)	K_m (mM)	V_{max} (units/mg)
WT	0.39 ± 0.13	116 ± 12	3.76 ± 0.51	110 ± 13
N15A	0.10 ± 0.01	0.39 ± 0.05	1.12 ± 0.21	0.57 ± 0.19
N15Q	2.66 ± 0.37	18 ± 0.87	3.91 ± 0.48	7.35 ± 0.62
R58A	0.83 ± 0.26	85 ± 8		
S19A	0.16 ± 0.04	0.38 ± 0.16	0.30 ± 0.13	0.27 ± 0.10
S43A	0.25 ± 0.08	68 ± 5		
H72A	0.31 ± 0.11	17 ± 0.95	1.5 ± 0.18	14 ± 0.72

[a] Measurements were made at pH 5.0, 37 °C, in 100 mM sodium acetate, 1 mM EDTA, and NaCl to give an ionic strength of 150 mM.

M., *et al.*, 1994; Zhou *et al.*, 1994). ^{1}H NMR spectra obtained during the course of urea denaturation of wild-type BPTP showed that these low-frequency resonances were undisturbed until urea concentration in excess of 4 M was reached (P. A. Tishmack, unpublished results), which is consistent with the urea denaturation experiments described elsewhere in the present study. Thus, the NMR results were consistent with the kinetic data and CD spectroscopy observed for the mutant proteins and indicate only minor, localized structural changes.

Steady-state Kinetics of BPTP Mutants. V_{max} and K_m values for *p*NPP and phenyl phosphate substrates were determined at pH 5.0 and 37 °C for the wild-type, N15A, N15Q, S19A, S43A, R58A, and H72A BPTP enzymes. These data are summarized in Table 1. The most striking results were seen for N15A and S19A. With the substrates *p*NPP and phenyl phosphate, the N15A mutant exhibited V_{max} values that were approximately 0.33% and 0.53% of that of WT BPTP, respectively, while S19A exhibited values of 0.33% and 0.25%, respectively. This is consistent with the hypothesis that both Asn-15 and Ser-19 serve important roles. For the S43A and R58A mutants, the kinetic parameters were only minimally affected, indicating that the side chains of these residues are not particularly important to the catalytic activity. Arg-58 is not involved in forming the P-loop structure but is instead a surface residue near the entrance to the active site and was selected as a probe of electrostatic effects. The R58A and N15Q mutants exhibited 2- and 7-fold increases in K_m, respectively. These results indicate that Asn-15 and Arg-58 serve in part to maintain the substrate binding affinity, albeit by different mechanisms.

For this phosphatase, it is known that substrate K_m values are generally not true equilibrium binding constants (Zhang & Van Etten, 1991b). To better compare changes in binding by the P-loop mutants, the dissociation constants K_i for inhibition by inorganic phosphate were measured for N15A, N15Q, R58A, and S19A as well as wild-type BPTP at pH 5.0. The measured K_i values for phosphate inhibition of wild-type, N15A, R58A, and S19A proteins were 1.8, 3.5, 5.8, and 6.2 mM, respectively. (Phosphate ion was such a poor inhibitor for N15Q that an accurate K_i could not be determined under comparable conditions. When high concentrations of substrate and inhibitor were used, the resulting increase in ionic strength caused a sharp rise in K_m and precluded saturation of the enzyme with the substrate.) The higher K_i values observed for the P-loop mutants N15A and S19A and for the mutant R58A reflect a reduced affinity for phosphate ion compared to the wild-type enzyme.

Scheme 1

$$E + pNPP \underset{k_{-1}}{\overset{k_1}{\rightleftharpoons}} E{\cdot}pNPP \underset{k_{-2}}{\overset{k_2}{\rightleftharpoons}} E{-}P + pNP \underset{k_{-3}}{\overset{k_3}{\rightleftharpoons}} E{\cdot}P \underset{k_{-4}}{\overset{k_4}{\rightleftharpoons}} E + P_i$$

Hydrolysis of Aryl Phosphomonoesters. BPTP catalyzes the hydrolysis of *p*NPP through the kinetic mechanism shown in Scheme 1. The rate-limiting step is normally dephosphorylation (Zhang & Van Etten, 1991b), and this typically results in constant V_{max} values regardless of the pK_a values of the aryl leaving group of the substrates. To assess whether the lower activity of the N15A, N15Q, H72A, and S19A mutants reflected a change in the rate-determining step of the catalytic mechanism from dephosphorylation of the phosphoenzyme intermediate to phosphorylation of the enzyme, several phosphomonoesters with significantly different leaving group pK_a values were tested (Table 2). For H72A, and N15A, the V_{max} values were effectively constant and parallel the kinetic results for wild-type enzyme. These results are consistent with dephosphorylation of the phosphoenzyme intermediate as the rate-limiting step in the catalytic mechanism (Zhang & Van Etten, 1991a). However, for S19A, the V_{max} value was significantly dependent on the leaving group pK_a (Figure 5), and the results were fitted to the linear relationship $\log V_{max} = 1.01 - 0.201pK_a$. This is consistent with a mechanism in which phosphorylation is the rate-limiting step. For the N15Q mutant, the K_m values were very high with several of the aryl phosphomonoesters. Consequently, it was not possible to accurately determine the leaving group dependence for this mutant.

Partitioning Experiments. A number of weakly acidic nucleophilic reagents including methanol, ethanol, and ethylene glycol, which can potentially act as acceptors of the phosphate group in place of water, are known to enhance the activity of wild-type BPTP (Zhang & Van Etten, 1991b; Zhang, Z., *et al*., 1994). For wild-type BPTP, a positive dependence was observed between the rate of release of *p*-nitrophenolate and the concentration of added methanol. At the same time, added methanol did not alter the corresponding rate of liberation of inorganic phosphate. Similar results have been described for the structurally unrelated *E. coli* acid phosphatase/phytase (Ostanin *et al*., 1993). Such experiments provide additional evidence that the rate-determining step of the reaction is hydrolysis of a phosphoenzyme intermediate.

In the present case, the behavior of the S19A mutant toward methanol was strikingly different from that observed for the wild-type enzyme. The V_{max} (as measured by release of *p*-nitrophenolate) did not vary in the presence of 0−2 M methanol (Figure 6). This result, along with the evidence from the leaving group dependence study, further supported the conclusion that phosphorylation of the enzyme became rate-limiting when Ser-19 was mutated to alanine.

Protein Stability Measurements. The unfolding of wild-type BPTP has been shown to closely approach a two-state folding mechanism (C. Pokalsky, unpublished results). The differences in conformational stability between WT BPTP and the P-loop mutants were determined by urea unfolding experiments. Analysis of each denaturation profile was performed by fitting the observed fluorescence intensities

Table 2: Michaelis−Menten Parameters for Hydrolysis of Aryl Phosphomonoesters[a]

phenyl phosphate ester	leaving group pK_a	WT		N15A		S19A		H72A	
		k_{cat} (s^{-1})	K_m (mM)	k_{cat} (s^{-1})	K_m (mM)	k_{cat} (s^{-1})	K_m (mM)	k_{cat} (s^{-1})	K_m (mM)
4-nitro	7.14	34.6 ± 3.6	0.39 ± 0.13	0.12 ± 0.015	0.10 ± 0.03	0.11 ± 0.048	0.16 ± 0.019	4.6 ± 0.59	0.31 ± 0.13
4-trifluoromethyl	8.68	28.0 ± 2.8	1.16 ± 0.23	0.20 ± 0.03	0.94 ± 0.25	0.059 ± 0.01	0.18 ± 0.043	4.5 ± 0.61	0.60 ± 0.25
β-naphthyl	9.38	28.2 ± 3.2	1.45 ± 0.18			0.040 ± 0.018	0.12 ± 0.034		
parent	9.99	34.6 ± 3.8	3.76 ± 0.37	0.17 ± 0.026	1.12 ± 0.15			4.3 ± 0.53	1.5 ± 0.23
4-ethyl	10.0	32.5 ± 2.9	2.99 ± 0.34	0.23 ± 0.035	0.76 ± 0.23	0.030 ± 0.007	0.30 ± 0.05	3.7 ± 0.38	1.0 ± 0.19

[a] Measurements were made at pH 5.0, 37 °C, in 100 mM sodium acetate, 1 mM EDTA, and NaCl added to give an ionic strength of 150 mM.

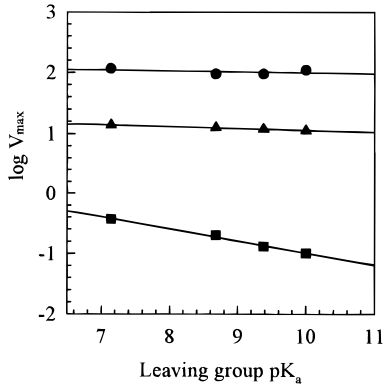

FIGURE 5: Effect of aryl phosphate leaving group pK_a on V_{max} for H72A (▲), S19A (■), and WT (●) BPTP. Activity was measured at 37 °C in 100 mM sodium acetate, pH 5.0, 1 mM EDTA, and 86.5 mM NaCl.

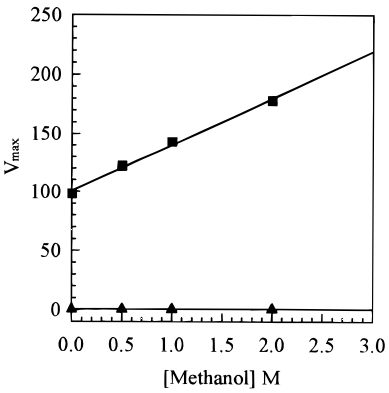

FIGURE 6: Effect of methanol on V_{max} for WT (■) and S19A (▲) BPTP. V_{max} was determined by measuring the liberation of *p*-nitrophenol at 37 °C in 100 mM sodium acetate, pH 5.0, 1 mM EDTA, and 86.5 mM NaCl.

to eq 3 (Pace *et al.*, 1989) using a nonlinear least squares analysis algorithm written in SigmaPlot (version 3.0, Jandel Scientific).

$$y_{obs} = [(y_n + m_n[D]) - (y_u + m_u[D])]/[1 + \exp[-((\Delta G_{H_2O} - m[D])/RT)]] + (y_u + m_u[D]) \quad (3)$$

Here, y_{obs} is the observed fluorescence intensity, y_n and y_u represent the fluorescence values characteristic of the folded and unfolded states, m_n and m_u are slopes that describe the folded and unfolded transitions, respectively, m is the slope of the unfolding transition, [D] is urea concentration, ΔG_{H_2O} is ΔG at 0 M urea, R is defined as 1.987 cal mol^{-1} K^{-1} and T is 298 K. The slope (m), a measure of transition steepness, reflects the structural differences of the native and unfolded states of the protein (Schellman, 1978). The m values for WT BPTP and the P-loop mutants ranged from 2310 to 2480 cal mol^{-1} M^{-1} with an average of 2460 ± 70 cal mol^{-1} M^{-1}.

Table 3: Parameters Characterizing the Urea Unfolding of Wild-Type and Mutant Forms of BPTP[a]

enzyme	$[urea]_{1/2}$ (M)	m (cal mol^{-1} M^{-1})	ΔG_{H_2O} (kcal/mol)	$\Delta(\Delta G)^b$ (kcal/mol)
WT	5.1	2480	10.3	
Y131A	5.5	2480	10.2	0.1
E139A	5.4	2470	9.9	0.4
S43A	4.8	2450	9.3	1.0
N15A	3.6	2530	6.6	3.7
H72A	3.5	2520	6.5	3.8
S19A	3.3	2310	5.0	5.3

[a] Measurements were made at pH 5.0, 25 °C, in 100 mM sodium acetate and 80 mM NaCl. [b] An experimental uncertainty of ±0.35 kcal/mol for $\Delta(\Delta G)$ values was estimated from the accumulated error in $[urea]_{1/2}$ (±0.1 M) and m (±70 cal mol^{-1} M^{-1}).

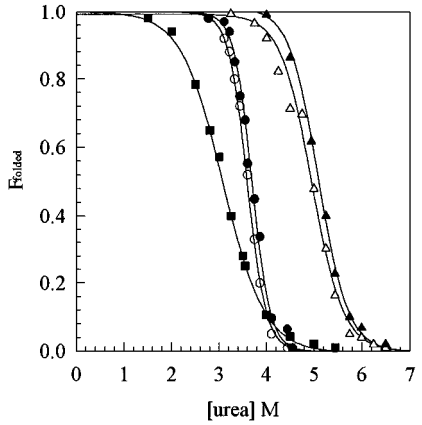

FIGURE 7: Fractional amount of folded protein, F_{folded}, as a function of urea molarity for wild-type BPTP (▲) and the mutants S43A (△), N15A (●), H72A (○), and S19A (■) at pH 5.0, 25 °C, in 100 mM sodium acetate buffer and 80 mM NaCl. Individual data series were fit to eq 3 as described in Experimental Procedures. Urea denaturation curves for Y131A and E139A BPTP were omitted for the sake of clarity, but they closely resemble the denaturation curve of wild-type BPTP.

The fact that none of the mutants had a slope value significantly different from that of WT BPTP indicated that these mutants also closely approach a two-state folding mechanism. Differences in the free energy change for unfolding in the absence of denaturant, ΔG_{H_2O}, for wild-type BPTP and P-loop mutants are given in Table 3. Typical results from urea denaturation experiments for several P-loop mutants are shown in Figure 7.

Effect of pH on k_{cat}/K_m. The pH dependence of k_{cat}/K_m for WT, S19A, and N15A BPTP each displayed a descending slope of −1, consistent with the known participation of a protonated residue during hydrolysis (Zhang, Z., *et al.*, 1994). For both S19A and N15A BPTP an ascending slope of approximately +2 was observed, consistent with the direct involvement of one unprotonated residue together with the monoanion of *p*NPP (Figure 8). The pK_a of the latter was

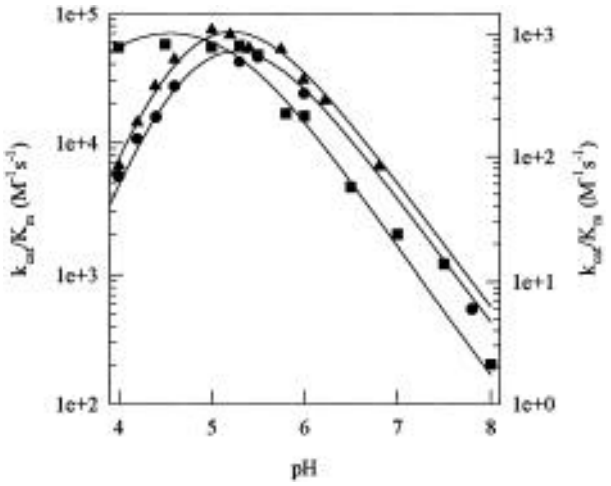

FIGURE 8: pH dependency of k_{cat}/K_m for WT BPTP (■) (left scale) and for N15A (▲) and S19A (●) (right scale). WT BPTP was fit to eq 2 while data for N15A and S19A were fit to eq 1 as described in Experimental Procedures.

held constant at 5.1 (Taga & Van Etten, 1982; Denu & Dixon, 1995). Due to the irreversible acid denaturation of WT BPTP at pH values ≤3.8, a comparable ascending slope could not be defined for WT BPTP (Figure 8). Consequently, the pK_a of Cys-12 in WT BPTP could not accurately be determined, but it was clearly below 4.0. Upon mutation of either Ser-19 or Asn-15 to alanine, the ascending curvature of the pH profile was shifted to higher pH, thus allowing for the interpretation of the ascending slope. The profiles for S19A and N15A BPTP both reflect an unprotonated residue with an approximate pK_a of 4.4, while the descending curvature reflected a protonated residue with a pK_a of 5.2, corresponding to the pK_a of Asp-129 (C. Pokalsky, unpublished results). The pK_a of the protonated residue derived from the descending slope of WT BPTP using eq 2 was determined to be 5.3, which is consistent with that observed for the two mutant proteins, S19A and N15A BPTP.

DISCUSSION

Recent structure determinations showed that several conserved residues, including Asn-15 and Ser-19, are directly involved in the formation of the active site phosphate binding loop of BPTP. In addition, a conserved histidine (His-72) and two conserved serines (Ser-19 and Ser-43) are located near the active site and appear to serve a function in stabilizing the active site loop by interacting with Asn-15. In order to assess the roles of these residues in the low molecular weight PTPases, specific mutants have now been constructed and analyzed. Asn-15 was replaced by glutamine and alanine, while Ser-19 and Ser-43 were replaced by alanine. Although all mutants retain phosphatase activity, several significant changes are observed. To test whether the reduced activity was due to a change in the catalytic mechanism from rate-determining dephosphorylation to phosphorylation, a series of aryl phosphomonoesters were tested. The activity of N15A, H72A, and wild-type enzymes showed no dependence on the leaving group pK_a of the aryl substrates tested. These results were consistent with the formation of a covalent phosphoenzyme intermediate and with the dephosphorylation of this intermediate as the rate-limiting step in the catalytic mechanism. In contrast, the activity of S19A showed a marked dependence on leaving group pK_a of the aryl substrates tested. This result suggested that the phosphorylation step was retarded to the point where it became rate-limiting. An independent procedure involving partitioning experiments also supported the conclusion that phosphorylation was rate-limiting for the S19A mutant.

Mutants at Asn-15 possessed different levels of activity depending on the amino acid substitution. The N15A mutant exhibited approximately 0.33% of the activity of wild-type enzyme at pH 5.0 with *p*NPP as the substrate, whereas N15Q had 15% of the activity, compared to wild-type enzyme under the same conditions. The active site loop may be distorted due to the extra methylene group of glutamine compared to the asparagine present in the wild-type enzyme, although the size of the additional methylene group may be partially accommodated by reorientation. Hence, glutamine may still be able to maintain the hydrogen-bonding network between His-72, Ser-19, and Ser-43. The N15Q mutant exhibited an 7-fold increase in K_m. This experimentally significant increase must be due at least in part to reduced true affinities for the substrate (i.e., increased K_s value), in view of the large increase in K_i for phosphate binding exhibited by this mutant. H72A also exhibited a significant reduction in V_{max} when *p*NPP was used as a substrate (Table 1).

Potential Roles for Ser-19, Asn-15, and His-72. Structural data for native BPTP suggest possible roles for Ser-19, His-72, and Asn-15 (Zhang, M., *et al.*, 1994). The hydroxyl group of Ser-19 is in very close proximity to the thiolate anion of Cys-12 (2.98 Å) and forms a hydrogen bond with this nucleophilic residue. Such an interaction is well-known in the case of many glutathione *S*-transferases (Wilce *et al.*, 1995). This hydrogen bond is one factor in causing the unusually low pK_a of Cys-12, which must be less than 4. By replacing the serine residue with alanine, the hydroxyl group of Ser-19 is eliminated, and the thiolate anion is no longer stabilized. This would be expected to increase the pK_a of the Cys-12 thiol, as shown by the altered k_{cat}/K_m curves in Figure 8. Moreover, the disruption of this hydrogen bond might also alter the geometry and/or conformation of the active site such that Cys-12 is no longer in an optimal position for nucleophilic attack on the substrate. For example, modeling studies suggest that, in the absence of a hydrogen bond to Ser-19, the thiolate anion might interact with the side chain of Arg-18. The normally rapid phosphorylation step (k_2) could then become rate-limiting. The catalytic rate constant is defined as $k_{cat} = k_2k_3/(k_2 + k_3)$ (Scheme 1). Therefore, when phosphorylation becomes rate-limiting, $k_3 \gg k_2$ and $k_{cat} \approx k_2$. The hypothesis that, in the S19A mutant, Cys-12 is no longer in an optimal position for nucleophilic attack and that the phosphorylation step is hindered was supported by the results of the leaving group dependence and partitioning experiments. Thus, Ser-19 appears to be important in stabilizing the thiolate anion of Cys-12 and in maintaining it in an optimal position for nucleophilic attack.

The present results are consistent with the hypothesis that Asn-15 also serves an important role in stabilizing the geometry of the active site loop region for optimal substrate binding and catalytic activity. In wild-type BPTP, Asn-15 is found in a strained (left-handed α-helical) conformation (Zhang, M., *et al.*, 1994, 1995). This energetically unfavorable conformation is stabilized by interaction of Asn-15 with His-72, Ser-19, and Ser-43. The hydrogen bonds between His-72, Ser-19, Ser-43, and Asn-15 all appear to serve

structural roles such that the active site loop can adopt the most favorable geometry for phosphate binding. The removal of the amide functionality in the N15A mutant disrupts the hydrogen-bonding network and would be expected to modify the P-loop conformation. The alanine residue is likely to adopt a normal right-handed conformation, which would be expected to alter the stability and geometry of the active site loop. The increased K_i for phosphate ion that is observed for N15A is also consistent with an altered, less favorable geometry for binding of phosphate ion or substrate.

The His-72 mutant has been studied extensively in our laboratory (Davis *et al.*, 1994a). His-72 is 8.4 Å from the active site nucleophile and is not directly involved in catalysis. However, it is a critical residue in the hydrogen-bonding network that forms the P-loop. Removal of this histidine residue decreased V_{max} to approximately 15% of that of the wild-type enzyme (Table 1).

Thermodynamic measurements of protein stability are also consistent with the importance of the hydrogen-bonding network involving P-loop residues. Strikingly large losses in structural stability are obtained for the N15A, H72A, and S19A mutants, as compared to small $\Delta(\Delta G)$ values for S43A, E139A, and Y131A (Table 3). The latter two mutants were selected as control proteins in which the site of mutation did not involve the P-loop or its directly associated hydrogen-bonding network. While these results cannot be interpreted with certainty until high-resolution structure determinations of the respective P-loop mutant proteins are available, the $\Delta(\Delta G)$ values are at least consistent with the loss of one hydrogen bond for S43A and the potential loss of two to three hydrogen bonds each for N15A, H72A, and S19A. Thus, kinetic, structural, and spectroscopic studies are all consistent with the conclusion that the disruption of hydrogen bonds in this network can greatly affect the activity of the enzyme.

The Ser-19 residue in BPTP is structurally analogous to Ser-131 in the dual-specificity phosphatase VHR (Denu & Dixon, 1995), but there are some clear differences in the roles of these residues in their respective enzymes. In VHR, the nucleophile Cys-124 has a low apparent pK_a of 5.6 ± 0.3 (Denu *et al*., 1995). However, removal of the hydroxyl group of Ser-131 did not shift the apparent pK_a of the nucleophile. Specifically, the S131A mutant reportedly showed no effect on the rate of formation of the phosphoenzyme intermediate or on the apparent pK_a of the nucleophilic cysteine (Denu & Dixon, 1995). In BPTP, the Ser-19 residue is important for facilitating ionization of the nucleophilic cysteine and probably for maintaining this residue in an orientation suitable for nucleophilic attack. This conclusion is supported by the shift in the apparent pK_a of Cys-12 in the S19A mutant as well as the change in the rate-determining step from dephosphorylation to phosphorylation.

The catalytic mechanism of BPTP can now be elaborated as follows. The catalytic nucleophile, Cys-12, attacks the phosphate substrate (e.g. *p*NPP) to form a phosphoenzyme intermediate. Concurrently, a proton is transferred from the proton donor Asp-129, leading to the release of phenolic product (Zhang, Z., *et al.*, 1994). The thiolate group of Cys-12 is held in place by a hydrogen bond to Ser-19 and thus positions the nucleophile for attack on the substrate. In the dephosphorylation step, the phosphoenzyme intermediate is attacked by a water molecule, releasing the second product,

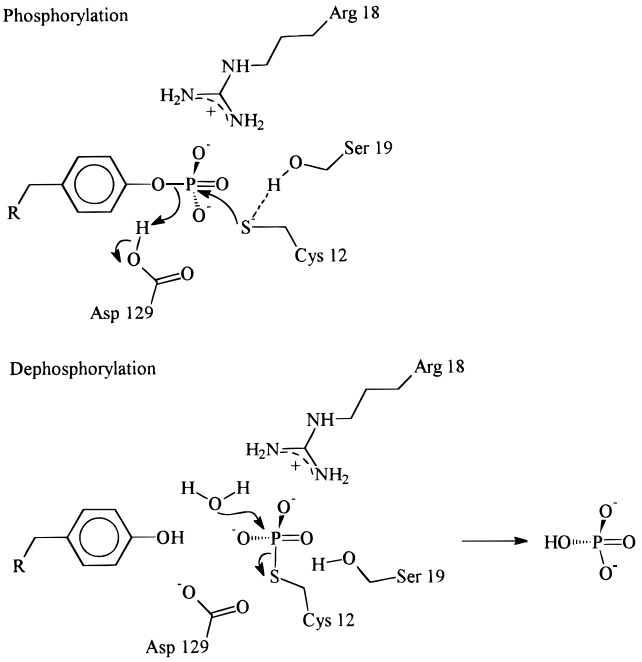

FIGURE 9: Catalytic mechanism for PTPases. As a proton is donated from the general acid Asp-129 to the leaving phenolic oxygen, the nucleophile Cys-12 attacks the phosphorylated substrate with the formation of a covalent phosphoenzyme intermediate. In a step that is normally rate-limiting, the phosphoenzyme subsequently reacts with water to form inorganic phosphate and regenerate the enzyme.

inorganic phosphate (Figure 9). Hydrogen bond interactions between the protein and the phosphate substrate, and between the protein and the phospho group of the phosphoenzyme, affect each of these steps. Moreover, as dephosphorylation proceeds, the thiolate anion leaving group is again increasingly stabilized by hydrogen bonding to the hydroxyl group of Ser-19. From the present work, it appears that the N15A mutation disrupts the hydrogen-bonding network which stabilizes the conformation of the phosphate binding loop of the enzyme and changes the geometry of this region. This substitution replaces a fairly large polar residue with a small hydrophobic residue. Substrate may enter the active site crevice more readily, but the rate of hydrolysis is slowed due to the destabilization of the active site loop by the disruption of hydrogen bonds. In addition, some of the stabilizing hydrogen bonds to the substrate and phosphoenzyme intermediate are altered or absent. As a consequence, the magnitudes of both ground-state and transition-state energies are altered, consistent with the changed K_m, K_i, and V_{max} values for the N15A mutant.

It will be of interest to probe additional, related interactions that are important to the specificity and mechanism of the enzyme. For example, previous pH titration studies revealed that the pK_as of the side chain imidazole groups of His-66 and His-72 are unusually high, 8.4 and 9.2, respectively, indicating that there is significant stabilization of the protonated form by interactions involving neighboring groups (Davis *et al*., 1994a; Zhou *et al*., 1993). Since His-72 interacts directly with Asn-15, one might expect a change in the pK_a of this histidine when the amide functionality is removed. Determination of the crystal structures of the N15A and S19A mutants, particularly using neutron diffraction techniques, would further define the roles of these residues.

ACKNOWLEDGMENT

We thank Dr. Kirill Ostanin for providing the sequence alignment figure and Prof. Shelley Copley for helpful discussions and references regarding glutathione *S*-transferases.

REFERENCES

Black, M. J., & Jones, M. E. (1983) *Anal. Biochem. 135*, 233−238.
Charbonneau, H., & Tonks, N. K. (1992) *Annu. Rev. Cell Biol. 8*, 469−493.
Chernoff, J., & Li, H. C. (1985) *Arch. Biochem. Biophys. 240*, 135−145.
Cohen, P. (1989) *Annu. Rev. Biochem. 58*, 453−508.
Cohen, P. (1992) *Trends Biochem. Sci. 17*, 408−413.
Davis, J. P., Zhou, M.-M., & Van Etten, R. L. (1994a) *Biochemistry 33*, 1278−1286.
Davis, J. P., Zhou, M.-M., & Van Etten, R. L. (1994b) *J. Biol. Chem. 269*, 8734−8740.
Denu, J. M., & Dixon, J. E. (1995) *Proc. Natl. Acad. Sci. U.S.A. 92*, 5910−5914.
Denu, J. M., Zhou, G., Guo, Y., & Dixon, J. E. (1995) *Biochemistry 34*, 3396−3403.
Edelman, A. M., Blumenthal, D. K., & Krebs, E. G. (1987) *Annu. Rev. Biochem. 56*, 567−613.
Fischer, E. H., Charbonneau, H., & Tonks, N. K. (1991) *Science 253*, 401−406.
Heinrikson, R. L. (1969) *J. Biol. Chem. 244*, 299−307.
Laemmli, U. K. (1970) *Nature 227*, 680−685.
Logan, T. M., Zhou, M.-M., Nettesheim, D. G., Meadows, R. P., Van Etten, R. L., & Fesik, S. W. (1994) *Biochemistry 33*, 11087−11096.
Okada, M., Owada, K., & Nakagawa, H. (1986) *Biochem. J. 239*, 155−162.
Ostanin, K., & Van Etten, R. L. (1993) *J. Biol. Chem. 268*, 20778−20784.
Ostanin, K., Pokalsky, C., Wang, S., & Van Etten, R. L. (1995) *J. Biol. Chem. 270*, 18491−18499.
Pace, C. N. (1986) *Methods Enzymol. 131*, 266−280.
Pokalsky, C., Wick, P., Harms, E., Lytle, F. E., & Van Etten, R. L. (1995) *J. Biol. Chem. 270*, 3809−3815.
Rehkop, D. M., & Van Etten, R. L. (1975) *Hoppe-Seyler's Z. Physiol. Chem. 356*, 1775−1782.
Sanger, F., Nicklen, S., & Coulson, A. R. (1977) *Proc. Natl. Acad. Sci. U.S.A. 74*, 5463−5467.
Schellman, J. (1978) *Biopolymers 17*, 1305−1322.
Schultz, G. E. (1992) *Curr. Opin. Struct. Biol. 2*, 61.
Stuckey, J. A., Schubert, H. L., Fauman, E. B., Zhang, Z.-Y., Dixon, J. E., & Saper, M. A. (1994) *Nature 370*, 571−575.
Su, X. D., Taddei, N., Stefani, M., Ramponi, G., & Norlund, P. (1994) *Nature 370*, 575−578.
Taga, E. M., & Van Etten, R. L. (1982) *Arch. Biochem. Biophys. 214*, 505−515.
Vandeyar, M. A., Weiner, M. P., Hutton, C. J., & Carl, A. (1988) *Gene (Amsterdam) 65*, 129−133.
Waheed, A., Laidler, P. M., Wo, Y.-Y. P., & Van Etten, R. L. (1988) *Biochemistry 27*, 4265−4273.
Wilce, M. C. J., Board, P. G., Feil, S. C., & Parker, M. W. (1995) *EMBO J. 14*, 2133−2143.
Wishart, D. S., & Sykes, B. D. (1994) *Methods Enzymol. 239*, 363−392.
Wishart, D. S., Sykes, B. D., & Richards, F. M. (1991a) *FEBS Lett. 293*, 72−80.
Wishart, D. S., Sykes, B. D., & Richards, F. M. (1991b) *J. Mol. Biol. 222*, 311−333.
Wo, Y.-Y. P., Zhou, M.-M., Stevis, P., Davis, J. P., Zhang, Z.-Y., & Van Etten, R. L. (1992a) *Biochemistry 31*, 1712−1721.
Wo, Y.-Y. P., McCormack, A. L., Shabanowitz, J., Hunt, D. F., Davis, J. P., Mitchell, G. L., & Van Etten, R. L. (1992b) *J. Biol. Chem. 263*, 6730−6737.
Zhang, M., Van Etten, R. L., & Stauffacher, C. V. (1994) *Biochemistry 33*, 11097−11105.
Zhang, M., Stauffacher, C., & Van Etten, R. L. (1995) *Adv. Protein Phosphatases 9*, 1−23.
Zhang, Z., Harms, E., & Van Etten, R. L. (1994) *J. Biol. Chem. 269*, 25947−25950.
Zhang, Z.-Y., & Van Etten R. L. (1990) *Arch. Biochem. Biophys. 282*, 39−49.
Zhang, Z.-Y., & Van Etten, R. L. (1991a) *Biochemistry 30*, 8954−59.
Zhang, Z.-Y., & Van Etten, R. L. (1991b) *J. Biol. Chem. 266*, 1516−1525.
Zhang Z.-Y., & Dixon, J. (1994) *Adv. Enzymol. 68*, 1−36.
Zhang, Z.-Y., Davis, J. P., & Van Etten, R. L. (1992) *Biochemistry. 31*, 1701−1711.
Zhou, M.-M., Davis, J. P., & Van Etten, R. L. (1993) *Biochemistry 32*, 3479−3486.
Zhou, M.-M., Logan, T. M., Thèriault, Y., Van Etten, R. L., & Fesik, S. W. (1994) *Biochemistry 33*, 5221−5229.

BI9605651